Molecular Biology of the Cell
Vol. 20, 4997–5006, December 1, 2009

Tight Functional Coupling of Kinesin-1A and Dynein Motors in the Bidirectional Transport of Neurofilaments

Atsuko Uchida,* Nael H. Alami, and Anthony Brown

Center for Molecular Neurobiology and Department of Neuroscience, The Ohio State University, Columbus, OH 43210

Submitted April 15, 2009; Revised August 14, 2009; Accepted September 29, 2009
Monitoring Editor: Erika L. Holzbaur

We have tested the hypothesis that kinesin-1A (formerly KIF5A) is an anterograde motor for axonal neurofilaments. In cultured sympathetic neurons from kinesin-1A knockout mice, we observed a 75% reduction in the frequency of both anterograde and retrograde neurofilament movement. This transport defect could be rescued by kinesin-1A, and with successively decreasing efficacy by kinesin-1B and kinesin-1C. In wild-type neurons, headless mutants of kinesin-1A and kinesin-1C inhibited both anterograde and retrograde movement in a dominant-negative manner. Because dynein is thought to be the retrograde motor for axonal neurofilaments, we investigated the effect of dynein inhibition on anterograde and retrograde neurofilament transport. Disruption of dynein function by using RNA interference, dominant-negative approaches, or a function-blocking antibody also inhibited both anterograde and retrograde neurofilament movement. These data suggest that kinesin-1A is the principal but not exclusive anterograde motor for neurofilaments in these neurons, that there may be some functional redundancy among the kinesin-1 isoforms with respect to neurofilament transport, and that the activities of the anterograde and retrograde neurofilament motors are tightly coordinated.

INTRODUCTION

Studies on cultured neurons using live-cell fluorescence imaging have demonstrated that neurofilament polymers move rapidly and intermittently along axons in both anterograde and retrograde directions (Roy *et al*., 2000; Wang *et al*., 2000; Wang and Brown, 2001; Uchida and Brown, 2004; Yan and Brown, 2005). The instantaneous rate of movement is fast, with peak velocities of up to 3.5 μm/s, but the overall rate is slow because the movements are interrupted by prolonged pauses (Brown, 2000, 2003; Brown *et al*., 2005; Trivedi *et al*., 2007). The rapid movement of neurofilaments in axons indicates that these cytoskeletal polymers are transported by fast motors, but the identity of these motors and the mechanism of movement are not well understood.

Several lines of evidence suggest that neurofilaments move along microtubule tracks, propelled by microtubule motor proteins (Prahlad *et al*., 2000; Shah *et al*., 2000; Francis *et al*., 2005), and that dynein/dynactin is the retrograde motor (Shah *et al*., 2000; Helfand *et al*., 2003; Wagner *et al*., 2004; He *et al*., 2005): 1) dynein and dynactin copurify with neurofilaments (Shah *et al*., 2000) and dynein/dynactin interacts with neurofilaments, possibly via an interaction between neurofilament protein M (NFM) and the dynein intermediate chain (Wagner *et al*., 2004); 2) knockdown of dynein heavy chain in cultured rat sympathetic neurons blocks retrograde neurofilament movement (He *et al*., 2005); and 3) dynein has also been shown to colocalize with peripherin in PC12 cells and overexpression of p50/dynamitin in those cells leads to a redistribution of peripherin to the distal regions of neurites, consistent with a selective inhibition of retrograde transport (Helfand *et al*., 2003).

Less is known about the anterograde motor for neurofilaments. Shea and colleagues have proposed that kinesin-1 is a neurofilament motor and that it interacts with the NFM and neurofilament protein H (NFH) subunits in a phosphorylation-dependent manner (Yabe *et al*., 1999, 2000; Jung *et al*., 2005). Kinesin-1 has been shown to colocalize with motile neurofilament particles in extruded squid axoplasm, as well as with vimentin and keratin containing structures in non-neuronal cells (Prahlad *et al*., 1998; Martys *et al*., 1999; Windoffer and Leube, 1999), and microinjection of a kinesin antibody into PC12 cells results in retention of neurofilaments in the cell body, and depletion of neurofilaments from the neurites (Helfand *et al*., 2003).

Kinesin-1 is a heterotetramer composed of two heavy chains and two light chains (Bloom *et al*., 1988; Kuznetsov *et al*., 1988; Johnson *et al*., 1990; Hirokawa and Takemura, 2005). Mammals have three kinesin-1 heavy chain genes: kinesin-1B, which is expressed ubiquitously, and kinesin-1A and kinesin-1C, which are expressed in neurons (Navone *et al*., 1992; Niclas *et al*., 1994; Xia *et al*., 1998). Consistent with its ubiquitous role, kinesin-1B knockout mice die in utero (Tanaka *et al*., 1998). In contrast, kinesin-1C knockout mice are viable, although they exhibit loss of some motor neurons and a slight decrease in overall brain size (Kanai *et al*., 2000). Recent evidence indicates that kinesin-1A, B, and C heavy chains form homodimers (DeBoer *et al*., 2008).

Additional evidence that kinesin-1 is a motor for neurofilaments has come from studies on kinesin-1A knockout mice by Goldstein and colleagues (Xia *et al*., 2003). The conventional knockouts (type I deletion) died shortly after birth, so the authors created conditional knockouts (type II deletion) by using a Cre-lox strategy. Cre recombinase ex-

This article was published online ahead of print in *MBC in Press* (http://www.molbiolcell.org/cgi/doi/10.1091/mbc.E09–04–0304) on October 7, 2009.

* Present address: Department of Developmental and Regenerative Medicine, Graduate School of Medicine, Mie University, 2-174 Edobashi Tsu, Mie 5148507, Japan.

Address correspondence to: Anthony Brown (brown.2302@osu.edu).

pression was driven by the synapsin-I promoter, which turns on several weeks postnatally. Three quarters of these mice exhibited seizures and died at around three weeks of age, but the remainder lived for at least 3 mo. These mice exhibited neurofilament accumulations in the soma of sensory neurons, a marked reduction in sensory axon caliber, but no apparent defect in the movement of a number of vesicle markers. Based on these data, the authors hypothesized that kinesin-1A is a motor for neurofilament transport. However, neurofilament transport was not studied directly.

In the present study, we have used live-cell fluorescence imaging in cultured neurons from wild type and kinesin-1A knockout mice to test directly the role of kinesin-1A and dynein/dynactin in neurofilament transport. Our data suggest that 1) kinesin-1A is the principal, but not exclusive, anterograde motor for neurofilaments; 2) kinesin-1A is necessary for retrograde as well as anterograde neurofilament movement; 3) there may be some functional redundancy among the kinesin-1 isoforms with respect to neurofilament movement; and 4) dynein/dynactin is required for anterograde as well as retrograde neurofilament movement. Thus there is a reciprocal interdependence between the anterograde and retrograde motors of neurofilament transport, which implies that the activities of these motors are tightly coordinated.

MATERIALS AND METHODS

Mice

Kinesin-1A +/− knockout mice were obtained from Dr. Larry Goldstein (Xia *et al*., 2003, type I deletion) and genotyped using the PCR primers described in that study. Homozygous kinesin-1A −/− and wild type kinesin-1A +/+ mice were obtained in the expected Mendelian proportions by crossing kinesin-1A +/− heterozygotes. For the experiments in Figures 1, 2, 3, 4, and 5, we used kinesin-1A −/− knockout mice and wild type kinesin-1A +/+ littermate controls. For the experiments in Figure 6, we used wild type ICR mice, obtained from Harlan (Indianapolis, IN).

Molecular Cloning

Mouse NFM (mNFM) cDNA (GenBank accession DQ201636) was obtained by reverse transcription-polymerase chain reaction (PCR) using RNA from wild-type P24 mouse cerebellum and subcloned into the pEGFP-C1 mammalian expression vector (Clontech, Mountain View, CA). The resulting pEGFP-mNFM expression vector coded for the codon-optimized F64L/S65T variant of green fluorescent protein fused to the amino terminus of mouse NFM by a 25-amino acid linker. Kinesin-1A cDNA (GenBank accession BC058396, I.M.A.G.E. clone 6824963) was obtained from American Type Culture Collection (Manassas, VA). Kinesin-1B and kinesin-1C cDNAs (GenBank accessions BC090841 and BC067051, I.M.A.G.E. clones 30543821 and 30536079) were obtained from Open Biosystems (Huntsville, AL). Each cDNA was subcloned into a pEGFP-C1 vector from which the enhanced green fluorescent protein (EGFP) sequence had been excised. All constructs were confirmed by sequencing. The hemagglutinin (HA)-tagged "dominant-negative" headless kinesin-1A, B, and C constructs were created by using PCR to amplify N-terminally truncated portions of the corresponding cDNAs and subcloned into the pCGN-HA mammalian expression vector of Tanaka and Herr (1990). The myc-tagged p50/dynamitin expression construct was obtained from Richard Vallee (Echeverri *et al*., 1996). The pDsRed-p150-CC1 expression construct, also known as pDsRed-p150$^{217–548}$, was obtained from Nick Quintyne (Quintyne and Schroer, 2002).

Cell Culture and Transfection

Primary cultures of neurons dissociated from superior cervical ganglia (SCG) and dorsal root ganglia (DRG) were obtained from newborn pups or embryonic day 18.5–19 embryos and cultured on glass coverslips coated with poly-D-lysine and Matrigel. The kinesin-1A +/+ and kinesin-1A +/− pups were viable but the kinesin-1A −/− pups displayed abnormal breathing and cyanosis and died shortly after birth, typically within 30 min (Xia *et al*., 2003). To allow time for genotyping, all cyanotic pups were killed immediately, and the ganglia were dissected and stored in Leibovitz's L15 medium on ice. This storage method had no adverse effect on the health or viability of the neurons. The remaining pups were maintained under a heat lamp for ~4–5 h. After obtaining the genotypes, ganglia were dissected from kinesin-1A +/+ pups and processed in parallel with kinesin-1A −/− ganglia that had been dissected earlier. Most of the cyanotic pups were found to be kinesin-1A −/−. The brains and DRG of wild-type and knockout littermates were similar in size, but the SCG were much smaller, containing only 20% of the wild-type cell number (data not shown). This suggests that kinesin-1A is required for the survival of many of the neurons in SCG or for the migration of SCG precursors earlier in development, but we have not investigated this further. Primary cultures of neurons dissociated from the cerebral cortex of neonatal mice were maintained at low density with a glial feeder layer using the sandwich technique of Banker and colleagues (Goslin *et al*., 1998). Human adrenal carcinoma SW13 cl.2 vim- cells were provided by Dr. Robert Evans (Sarria *et al*., 1994) and cultured in DMEM/F-12 medium (Invitrogen, Carlsbad, CA) supplemented with 5% fetal bovine serum and 10 μg/ml gentamicin and maintained at 37°C/5% CO_2 in a humidified atmosphere. SCG neurons were transfected 1–2 d after plating by nuclear injection with 20 μg/ml DNA. Cortical neurons were transfected in suspension before plating by electroporation with 25 or 75 μg/ml DNA by using an Amaxa Nucleofector (Lonza Cologne AG, Koeln, Germany). SW13 vim- cells were transfected using Lipofectamine 2000 (Invitrogen) according to the manufacturer's protocol.

Antibody Injections

Mouse monoclonal antibody (mAb) IC74.1 (Dillman and Pfister, 1994) was purified from tissue culture supernatant by high-performance liquid chromatography on a recombinant protein G column and then dialyzed against phosphate-buffered saline (PBS) and stored at −80°C. To prepare the antibody for microinjection, we dialyzed it against 50 mM potassium glutamate, pH 7.2, and then concentrated it to 3 mg/ml in a Microcon centrifugal concentrator (Millipore, Billerica, MA). To investigate the effect of the antibody on neurofilament transport, we first transfected neurons with green fluorescent protein (GFP)-tagged NFM by nuclear injection (see above) after 2 d in culture. Three days later, we injected the same cells a second time, this time into the cytoplasm, with a mixture of 2.4 mg/ml antibody plus 1.5 mg/ml tetramethylrhodamine-labeled dextran (M_w 10,000; Sigma-Aldrich, St. Louis, MO). Movies were acquired 2–6 h after injection. All microinjections were performed using an Eppendorf FemtoJet with InjectMan three-axis motorized micromanipulator (Brinkmann Instruments, Westbury, NY).

RNA Interference (RNAi)

Three small interfering RNA (siRNA) oligonucleotide duplexes targeting nonoverlapping regions of mouse dynein heavy chain mRNA were purchased from Invitrogen (catalog no. 1320003, Stealth Select 3 RNAi). The sequences were 1) 5′-GAG GCU UCG GCA GUA UGC UUC CUA U-3′ and 5′-AUA GGA AGC AUA CUG CCG AAG CCU C-3′, 2) 5′-CCG GCG UUU CCA GCA UCA UCU UAA A-3′ and 5′-UUU AAG AUG AUG CUG GAA ACG CCG G-3′, and 3) 5′-GAG UGU GCU UGU AAG UGC AGG CAA U-3′ and 5′-AUU GCC UGC ACU UAC AAG CAC ACU C-3′. For control experiments, we used the Stealth RNAi Negative Control Duplex with medium GC content (catalog no. 12935300; Invitrogen). The lyophilized oligonucleotide duplexes were reconstituted to 20 μM in diethyl pyrocarbonate-treated water and then diluted to 100 nM in 50 mM potassium glutamate, pH 7.2. The siRNAs were microinjected into the cytoplasm of neurons after 1 d in culture, and then the following day the same neurons were transfected with GFP-tagged NFM by nuclear injection as described above. Neurofilament movement was analyzed 5 d later (i.e., after 7 d in culture) as described below.

Microscopy, Imaging, and Motion Analysis

Cells were observed by epifluorescence and phase contrast or differential interference contrast microscopy on a Quantum TE300 or TE2000 inverted microscope (Nikon, Garden City, NY) by using a Nikon 100×/1.4 numerical aperture Ph3 Plan Apo phase contrast or differential interference contrast oil immersion objective and fluorescein isothiocyanate/EGFP or tetramethylrhodamine B isothiocyanate filter sets (HQ 41001 and 41002b, respectively; Chroma Technology, Brattleboro, VT). Images were acquired using Micromax 512BFT or CoolSNAP HQ cooled charge-coupled device cameras (Roper Scientific, Trenton, NJ) and MetaMorph software (Molecular Devices, Sunnyvale, CA). The movement of neurofilaments was observed by time-lapse imaging in naturally occurring gaps in the axonal neurofilament array as described previously (Wang *et al*., 2000). The epifluorescent illumination was attenuated eightfold by using neutral density filters, and images were acquired with 1-s exposures at 4-s intervals. All movies were 15 min in length. The observation medium consisted of Hibernate-E (BrainBits, Springfield, IL) supplemented with B27 supplement mixture (Invitrogen), 0.3% glucose, 1 mM L-glutamine, 66 mM NaCl, and 100 ng/ml 2.5S nerve growth factor (BD Biosciences, San Jose, CA). Motion analysis was performed by tracking the position of the leading or trailing ends of the filaments in successive frames of the time-lapse image movies by using MetaMorph software. All objects greater than or equal to 10 pixels (1.31 μm) in length were analyzed if they moved a total distance of at least 25 pixels (3.275 μm) and could be tracked through at least three successive frames of the movie. Sustained reversals were defined as changes in direction that persisted for at least 70 pixels (9.17 μm) and at least 24 s. For the small number of neurofilaments that exhibited a sustained reversal, the anterograde and retrograde phases were considered to be separate bouts of movement and were analyzed separately. The frequency of neurofilament movement for a given treatment or condition was

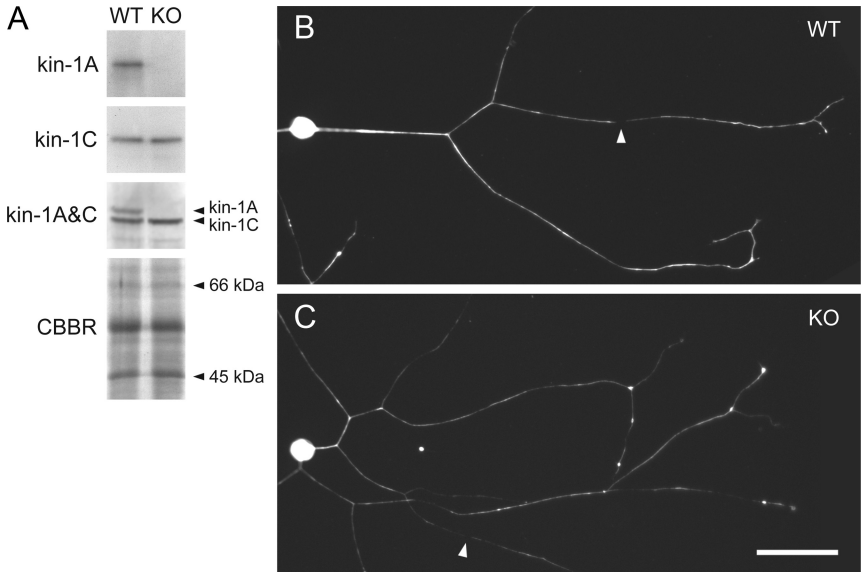

Figure 1. Neurons from kinesin-1A knockout mice extend axons containing neurofilaments. (A) Western blotting of total brain protein from wild-type (WT) and kinesin-1A knockout (KO) littermates, confirming the absence of kinesin-1A. Kinesin-1A and kinesin-1C were detected using affinity purified antisera. Mixing these two antisera (kinesin-1A&C) confirmed the absence of kinesin-1A because kinesin-1A migrates more slowly than kinesin-1C by SDS-PAGE. To demonstrate equivalent protein content of the two samples, we show a portion of a gel stained with Coomassie Brilliant Blue R (CBBR). (B) Cultured SCG neurons from wild type and kinesin-1A knockout mouse littermates after 12 h in culture, immunostained with a polyclonal antibody against neurofilament protein L. Neurofilaments extended throughout the axons of both wild-type and knockout neurons, occasionally interrupted by short gaps (for example, see white arrowheads). Bar, 50 μm.

expressed as the number of neurofilaments meeting the above criteria which moved into or through the field of view per minute or per 15-min movie, averaged over all the movies analyzed.

Western Blotting

For Western blotting of kinesin and dynein/dynactin proteins, mouse brains from embryonic day 18.5–19 pups were homogenized in cold 2× sample buffer (0.125 M Tris-HCl, pH 6.8, 4% SDS, 20% glycerol, and 10% 2-mercaptoethanol), heated for 5 min at 95°C, and then centrifuged at 15,000 × *g* for 15min at room temperature. The supernatants were diluted twofold with water and subjected to SDS-polyacrylamide gel electrophoresis. For Western blotting of full-length or headless kinesin-1 constructs, SW13 vim- cells expressing these proteins were harvested in cold 2× sample buffer and then processed in the same way. Kinesin-1A and kinesin-1C were detected using affinity-purified antisera provided by Larry Goldstein (Xia *et al.*, 2003). Full-length and headless kinesin-1 constructs were detected using mAb H2 (MAB 1614; Millipore Bioscience Research Reagents, Temecula, CA). Dynein intermediate chain, p150/135, and p50 were detected using polyclonal antibodies obtained from Erica Holzbaur (UP1467, UP235, and UP1097, respectively). Neurofilament protein M was detected using mAb RMO255 from V. Lee (University of Pennsylvania, Philadelphia, PA). Dynein heavy chain was detected using polyclonal antibody R-325 (Santa Cruz Biotechnology, Santa Cruz, CA). Blots were stained with secondary antibody conjugated to alkaline phosphatase or horseradish peroxidase (Jackson ImmunoResearch Laboratories, West Grove, PA) and visualized using the 5-bromo-4-chloro-3-indolyl phosphate/nitro blue tetrazolium phosphatase substrate system (Kirkegaard and Perry Laboratories, Gaithersburg, MD) or the ECL Plus chemiluminescent Western blotting detection reagent (GE Healthcare, Little Chalfont, Buckinghamshire, United Kingdom), respectively. Protein concentration was determined with a Coomassie Blue protein assay reagent (Pierce Chemical, Rockford, IL).

Immunostaining and Quantification of Fluorescence

Cultures were fixed with a solution containing 4% (wt/vol) paraformaldehyde and 1% sucrose in PBS and then demembranated by treatment with 0.1% Triton X-100 and processed for immunostaining using standard methods. Blocking was performed using 4% normal goat serum (Jackson ImmunoResearch Laboratories) and 5% fat-free milk in PBS ("blocking solution"). Neurofilament protein L was detected using a polyclonal antibody from V. Lee. HA tags were visualized using a mouse mAb (clone 12CA5; Covance Research Products, Princeton, NJ). Dynein heavy chain, dynein intermediate chain, and neurofilament protein M were visualized using the same antibodies that we used to detect these proteins on Western blots (see above). Secondary antibodies were goat anti-mouse immunoglobulin G (IgG) or goat anti-rabbit IgG conjugated with Alexa 488 or Alexa 568 (Invitrogen). To quantify the expression level of HA-tagged kinesin-1 constructs or the extent of knockdown of dynein heavy chain, we immunostained neurons with HA or dynein heavy chain antibody (see above) and measured the fluorescence intensities in neuronal cell bodies using MetaMorph software. To correct for background fluorescence and for any nonspecific staining, we used the average pixel intensity of randomly selected cell bodies of nontransfected neurons in the same culture dishes.

RESULTS

Western blotting of brain homogenates demonstrated that kinesin-1A was absent in kinesin-1A knockout mice, whereas the other neuron-specific kinesin-1 isoform, kinesin-1C, was unchanged (Figure 1A). Cultured neurons from SCG and dorsal root ganglia (DRG) of these knockout mice extended axons of comparable length and morphology to wild type, and both wild-type and knockout axons contained neurofilaments along their entire length (Figure 1, B and C). After 12 h in culture, the knockout axons seemed thinner than wild-type axons, but by 24 h this difference was no longer apparent. The presence of neurofilaments along the axons of both SCG and DRG neurons in the absence of kinesin-1A indicates that if kinesin-1A is an anterograde motor for neurofilament transport, it cannot be the only motor with this capability.

Cultured SCG neurons exhibit discontinuities in the neurofilament array, which we have termed naturally occurring gaps (Wang *et al.*, 2000, also see Figure 1, B and C). To study the role of kinesin-1A in neurofilament transport, we transfected cultured SCG neurons from wild-type and kinesin-1A knockout mice with GFP-tagged NFM after 1 to 2 d in culture and then observed neurofilament movement through these gaps 3 d later using time-lapse fluorescence imaging. The most striking difference between the knockout and wild-type neurons was a 75% reduction in the frequency of neurofilament movement in both anterograde and retrograde directions, from 0.105 and 0.116 neurofilaments/min, respectively, in the wild type to 0.027 and 0.029 neurofilaments/min, respectively, in the knockout (Figure 2A; Supplemental Movies 1 and 2). In both cases this reduction was statistically significant (Supplemental Table S2). However, it is important to note that some neurofilaments did move in the knockout neurons, albeit much less frequently than in the wild type (Supplemental Movies 3 and 4). Thus these data are consistent with a role for kinesin-1A as an anterograde neurofilament motor but they indicate that kinesin-1A cannot be the sole anterograde motor. In addition, these data suggest that kinesin-1A is also required for retrograde neurofilament movement.

To confirm that the decreased frequency of neurofilament movement in the kinesin-1A knockout neurons was due to

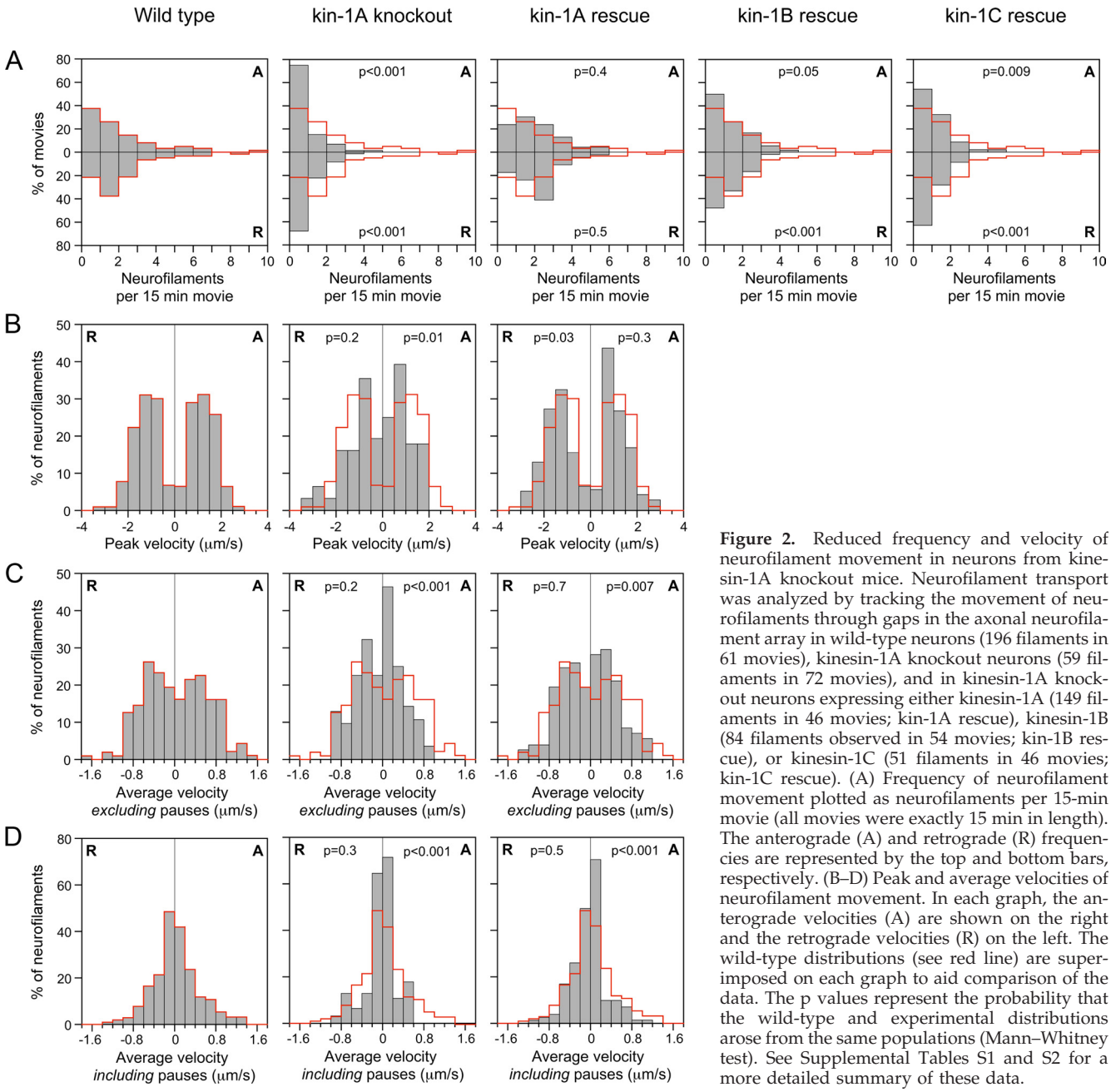

Figure 2. Reduced frequency and velocity of neurofilament movement in neurons from kinesin-1A knockout mice. Neurofilament transport was analyzed by tracking the movement of neurofilaments through gaps in the axonal neurofilament array in wild-type neurons (196 filaments in 61 movies), kinesin-1A knockout neurons (59 filaments in 72 movies), and in kinesin-1A knockout neurons expressing either kinesin-1A (149 filaments in 46 movies; kin-1A rescue), kinesin-1B (84 filaments observed in 54 movies; kin-1B rescue), or kinesin-1C (51 filaments in 46 movies; kin-1C rescue). (A) Frequency of neurofilament movement plotted as neurofilaments per 15-min movie (all movies were exactly 15 min in length). The anterograde (A) and retrograde (R) frequencies are represented by the top and bottom bars, respectively. (B–D) Peak and average velocities of neurofilament movement. In each graph, the anterograde velocities (A) are shown on the right and the retrograde velocities (R) on the left. The wild-type distributions (see red line) are superimposed on each graph to aid comparison of the data. The p values represent the probability that the wild-type and experimental distributions arose from the same populations (Mann–Whitney test). See Supplemental Tables S1 and S2 for a more detailed summary of these data.

the absence of kinesin-1A protein, we performed rescue experiments (Figure 2A and Supplemental Movie 5). In knockout neurons transfected with kinesin-1A, the average frequencies of movement were 0.104 neurofilaments/min in the anterograde direction and 0.112 neurofilaments/min in the retrograde direction, which corresponds to 99 and 97% of the wild-type frequency, respectively. Statistical analysis revealed no significant difference from wild type, indicating that kinesin-1A was capable of rescuing the frequency of both anterograde and retrograde neurofilament movement in the knockout (Supplemental Table S2). To examine the specificity of this rescue effect, we also transfected kinesin-1A knockout neurons with kinesin-1B and kinesin-1C. In knockout neurons expressing kinesin-1B, the average frequency of movement in the anterograde and retrograde directions was 53 and 41% of wild type, respectively, whereas in knockout neurons expressing kinesin-1C, it was 41 and 25% of wild type, respectively. Statistical analysis of these data indicated that kinesin-1B and kinesin-1C partially rescued the frequency of both anterograde and retrograde neurofilament movement in the kinesin-1A knockout neurons, but with successively decreasing efficacy (Supplemental Table S2). Thus, kinesin-1B and C may also be capable of moving neurofilaments in these axons, but kinesin-1A seems to be the preferred motor. These data are summarized in Figure 3A.

To probe the role of kinesin-1A in neurofilament transport further, we analyzed the moving and pausing behavior of neurofilaments in wild-type and kinesin-1A knockout neurons and in kinesin-1A knockout neurons expressing kinesin-1A (kinesin-1A rescue) in more detail. The neurofilaments exhibited infrequent bouts of rapid movement

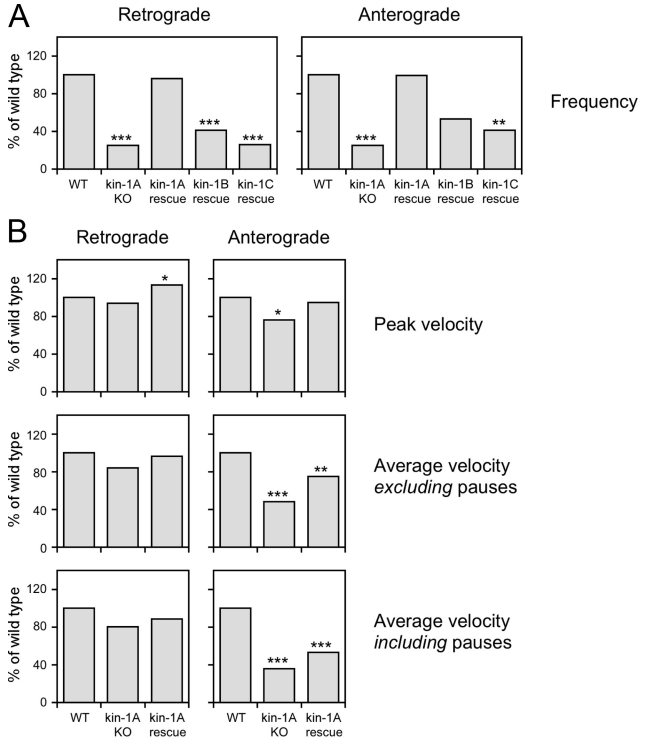

Figure 3. Summary of kinetic data. (A) Bar graphs showing the mean frequency of neurofilament movement in wild-type neurons (WT); in kinesin-1A knockout neurons (kin-1A KO); and in kinesin-1A knockout neurons expressing kinesin-1A (kin-1A rescue), kinesin-1B (kin-1B rescue), or kinesin-1C (kin-1C rescue), each normalized to the mean in the wild type. (B) Bar graphs showing the mean peak velocity and mean average velocity including or excluding pauses for wild-type neurons (WT), kinesin-1A knockout neurons (kin-1A KO), and for kinesin-1A knockout neurons expressing kinesin-1A (kin-1A rescue), each normalized to the mean in the wild type. The asterisks denote probability that the wild-type and experimental distributions arose from the same populations (Mann–Whitney test: ***$p < 0.005$, **$p < 0.01$, and *$p < 0.05$). See Supplemental Tables S1 and S2 for a more detailed summary of these data.

interrupted by prolonged pauses, as described previously (Wang *et al.*, 2000). In neurons from kinesin-1A knockout mice, there was a shift toward lower peak velocities for both anterogradely and retrogradely moving neurofilaments, but this was only found to be statistically significant in the anterograde direction (Figure 2B and Supplemental Table S2). Expression of kinesin-1A in the knockout neurons rescued the anterograde peak velocities and actually increased the retrograde peak velocities above that of the wild type. The average retrograde velocities excluding and including pauses were reduced slightly in the knockout, and this was reversed by expression of kinesin-1A, but these differences were not statistically significant (Figures 2, C and D, and Supplemental Table S2). In contrast, the average anterograde velocities excluding and including pauses were reduced to 48 and 35% of wild type, respectively, and these differences were statistically significant. Expression of kinesin-1A increased the average anterograde velocities in the knockout, but the data were still significantly different from the wild type, indicating that the extent of rescue was only partial. In conclusion, the absence of kinesin-1A resulted in a significant reduction in anterograde velocity, but no significant change in retrograde velocity, and the reduction in anterograde velocity could be rescued partially by kinesin-1A. These data are summarized in Figure 3B.

The above-mentioned data suggest that kinesin-1A is required for both anterograde and retrograde transport of neurofilaments in cultured SCG neurons and that there may be some functional redundancy among the kinesin-1 isoforms. To confirm these conclusions, we made headless (putative dominant negative) constructs of kinesin-1A, B, and C and investigated their effect on neurofilament transport in SCG neurons from wild-type mice. Headless kinesin-1A and kinesin-1C inhibited neurofilament transport in both anterograde and retrograde directions in a concentration-dependent manner and with similar efficacy (Figure 4). The highest levels of expression inhibited both anterograde and retrograde movement by 88–95%. Notably, this level of inhibition was greater than we observed in the kinesin-1A knockout neurons, which suggests that both kinesin-1A–dependent and kinesin-1A–independent movement was affected. Expression of headless kinesin-1B also seemed to inhibit both anterograde and retrograde neurofilament transport, but it resulted in poor cell viability so the data are not shown.

One possible explanation for the defect in retrograde neurofilament movement in the above-mentioned experiments is that kinesin-1A could be responsible for delivering dynein/dynactin motors to the axon and the defect in retrograde neurofilament movement could be due to a depletion of the retrograde motor from the axons. To test this hypothesis, we investigated the expression and localization of dynein and dynactin proteins in the absence of kinesin-1A. Western blotting of total brain protein revealed no difference between wild-type and kinesin-1A knockout littermates in the expression level of several different dynein and dynactin subunits (Figure 5A). Immunostaining of cultured SCG neurons from wild-type and knockout littermates revealed no apparent reduction in the amount of dynein intermediate chain in distal axons (Figure 5, B and D), and similar results were also obtained for p50/dynamitin, p150, and dynein heavy chain (data not shown). To confirm this quantitatively, we transfected wild-type neurons with headless kinesin-1A and then quantified the amount of dynein intermediate chain in the distal axons by immunofluorescence microscopy. The background-corrected fluorescence intensity in the most distal 50 μm of the axons (including the growth cone) was actually greater in neurons expressing the headless construct (average = 479 ADU/pixel, n = 119) than in the wild type (average = 301 ADU/pixel, n = 120), and this difference was significantly different ($p < 0.001$, Mann–Whitney test). Similar results were obtained when the growth cone was excluded from the measurement region. The reason for the increase is unclear, but certainly these data do not support the hypothesis that kinesin-1A is required for delivering dynein/dynactin to axons.

These data suggest that kinesin-1A is required for the retrograde transport of neurofilaments. One possible explanation for this is that the activities of the anterograde and retrograde motors are coupled such that the activity of kinesin-1A is required for the activity of dynein. If this is the case, then we might expect that the converse would also be true and that dynein/dynactin might also be required for anterograde neurofilament movement. However, knockdown of dynein heavy chain by RNAi has been reported to inhibit retrograde neurofilament movement selectively without inhibiting anterograde movement (He *et al.*, 2005), which suggests that the anterograde and retrograde motors are independent. To confirm these observations, we attempted to reproduce the dynein heavy chain RNAi result in

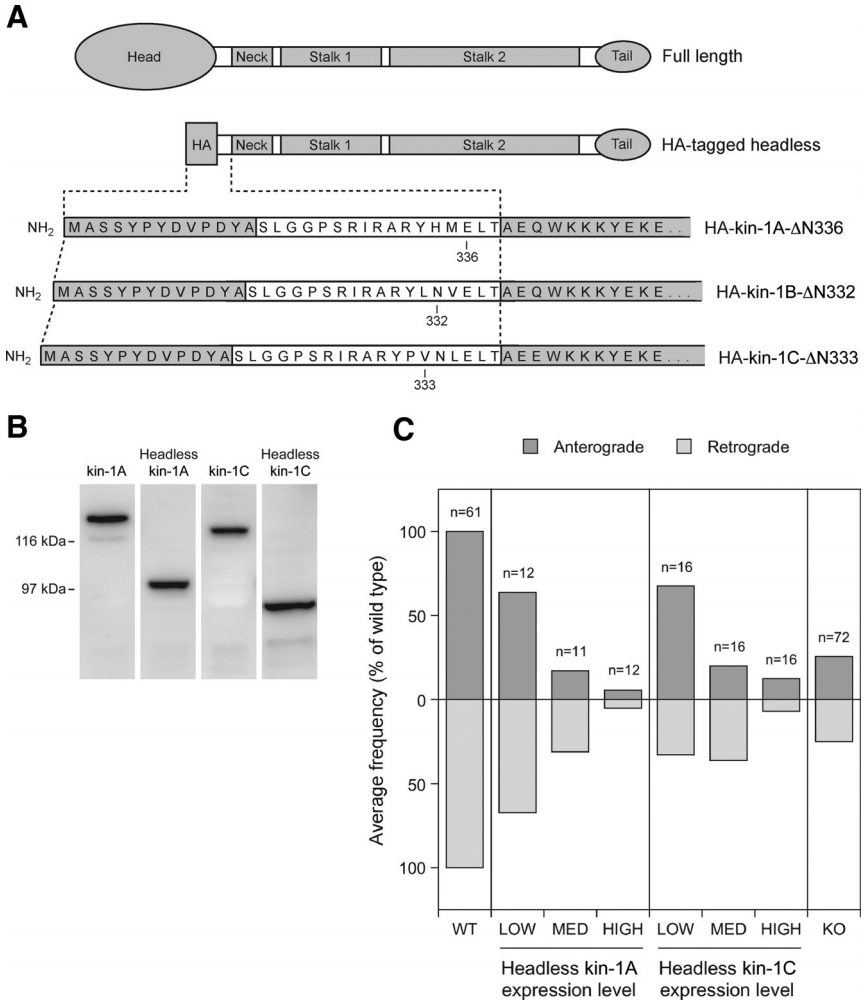

Figure 4. Headless kinesin-1A and kinesin-1C inhibit movement in both directions. (A) Schematic illustration of the structure of the headless kinesin-1A, B, and C constructs. Each construct was created by replacing the N-terminal head domain with an HA epitope tag, but retaining the entire tail, stalk, and neck domains and a portion of the neck linker (Kozielski *et al*., 1997). The sequence MASSYPYDVPDYA is the HA tag and the sequence SLGGPSRIRARY in the linker comes from the multiple cloning site of the HA vector. Kinesin-1A is truncated at amino acid 336, kinesin-1B at amino acid 332, and kinesin-1C at amino acid 333. (B) Western blot of extracts from cultured SW13 cells expressing full-length and headless kinesin-1A and C constructs, stained with mAb H2. The apparent molecular masses are ~131 and 98 kDa for full-length and HA-tagged headless KIFA, respectively, and ~122 and 92 kDa for full-length and HA-tagged headless KIFC, respectively. (C) Cultured SCG neurons from wild-type mice were cotransfected by nuclear injection with GFP-NFM and either HA-tagged headless kinesin-1A or HA-tagged headless kinesin-1C. Neurofilament transport was analyzed by time-lapse fluorescence imaging of gaps. To correlate the extent of neurofilament movement with the level of headless construct expression, we fixed the cultures after live-cell imaging and processed them for immunostaining using antibodies against NFM and the HA tag (see *Materials and Methods*). The bar graphs show the correlation between the average frequency of neurofilament movement (normalized to the frequency in the wild type) and the expression level of the headless construct. The anterograde and retrograde frequencies are represented by the top and bottom bars, respectively. The average frequency of movement in the wild type (WT) and kinesin-1A knockout (KO) in the absence of headless construct are included for comparison.

SCG neurons from wild-type mice. We observed a 76% reduction in the level of dynein heavy chain and a reduction in the frequency of retrograde and anterograde movements by 54 and 66%, respectively (Figure 6, A and B). We also microinjected SCG neurons with a mAb to dynein intermediate chain (clone IC74.1) (Dillman and Pfister, 1994), which has been shown to block dynein function in a variety of different studies (Leopold *et al*., 2000; Vorobjev *et al*., 2001; Lakadamyali *et al*., 2003). Two to 6 h after injection we observed a reduction in retrograde and anterograde frequency of 74 and 85%, respectively (Figure 6C).

To confirm these data using a dominant-negative strategy, we transfected SCG neurons with myc-tagged chicken dynamitin, which disrupts dynein function by dissociating the dynactin complex (Echeverri *et al*., 1996; Melkonian *et al*., 2007). The viability of the cells was poor, but in those cells that were viable we observed a reduction in retrograde and anterograde frequency of 62 and 56% respectively (Figure 6D). Finally, we transfected cortical neurons with DsRed-tagged coiled coil 1 (CC1) domain of p150, which is a subunit of dynactin. Previous studies have shown that overexpression of this construct disrupts dynein function in a dominant-negative manner by dissociating dynein from the dynactin complex (Quintyne and Schroer, 2002). In cells transfected by electroporation with a 75 μg/ml concentration of the expression construct we observed a reduction in retrograde and anterograde frequency of 66 and 72%, respectively, after 2 d in culture and a reduction of 71 and 70%, respectively, after 4 d in culture. In cells transfected with a 25 μg/ml concentration of the expression construct, we observed a reduction in retrograde and anterograde frequency of 46 and 31%, respectively, after 2 d in culture and a reduction of 81 and 75%, respectively, after 4 d in culture, although in this case the reduction after 2 d in culture was not statistically significant. Thus, in our hands, four independent perturbations of dynein function in two different neuronal cell types all resulted in a reciprocal inhibition of anterograde and retrograde movement. Notably, there was remarkable symmetry in the extent of inhibition in these experiments, with the frequency of anterograde neurofilament movement largely mirroring the frequency in the retrograde direction, regardless of the extent of inhibition.

DISCUSSION

The proposal that kinesin-1A is an anterograde motor for neurofilaments was based primarily on the observation that DRG neurons of conditional kinesin-1A knockout mice exhibit perikaryal neurofilament accumulations and a reduction in axonal caliber (Xia *et al*., 2003), but neurofilament transport was not measured directly. Our own data now provide direct evidence that kinesin-1A is an anterograde motor for neurofilaments and that it is the principal motor, at least in SCG neurons. However, the persistence of some

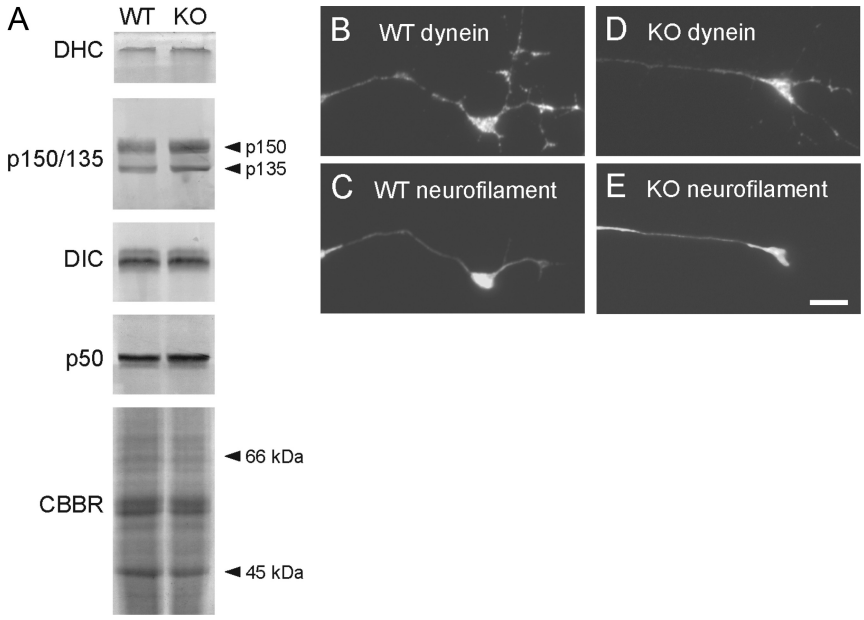

Figure 5. Dynein and dynactin levels are normal in brains and in axons of cultured neurons from kinesin-1A knockout mice. (A) Western blot of total brain proteins from wild-type (WT) and kinesin-1A knockout (KO) mice obtained with antibodies specific for dynein heavy chain (DHC), dynein intermediate chain (DIC), and the p150/135 and p50 subunits of dynactin. To demonstrate equivalent protein content of the two samples, we show a portion of a gel stained with Coomassie Brilliant Blue R (CBBR). (B–E) Immunostaining of wild-type and knockout SCG neurons using antibodies specific for dynein intermediate chain (B and D) and neurofilament protein M (C and E). Bar, 5 μm.

anterograde neurofilament movement in the kinesin-1A knockout neurons indicates that kinesin-1A cannot be the only motor with this capability. Indeed, whereas the axonal neurofilament content seemed to be slightly reduced in kinesin-1A knockout neurons after 12 h in culture, by 1 d in culture it was indistinguishable from the wild type. Thus, the neurofilament movement that persisted in the absence of kinesin-1A was sufficient to transport neurofilaments into the axons, albeit less efficiently.

The identity of the other anterograde motor(s) is unclear, but kinesin-1B and kinesin-1C are possible candidates because both were capable of rescuing neurofilament transport partially in kinesin-1A knockout neurons. In addition, headless kinesin-1C disrupted neurofilament movement in wild-

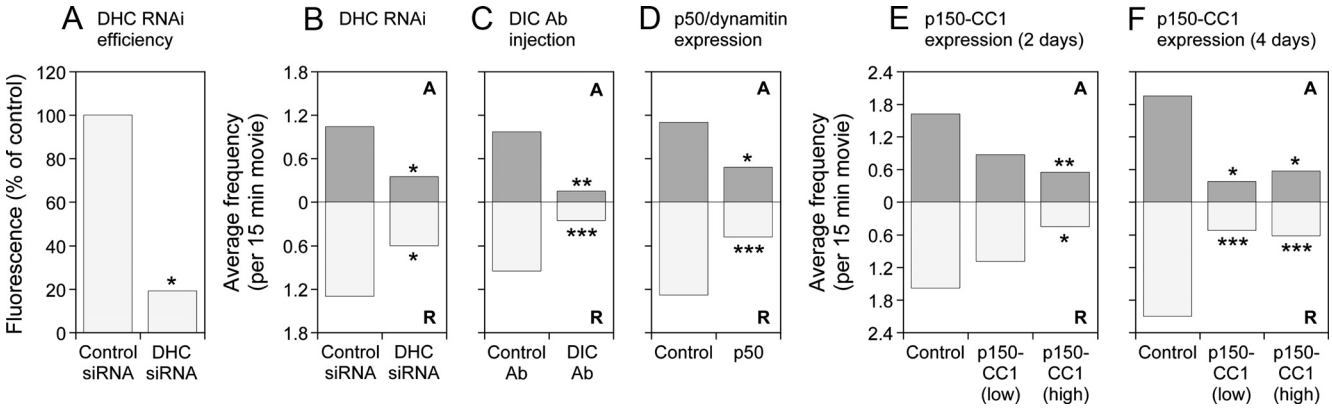

Figure 6. Disruption of dynein/dynactin inhibits both anterograde and retrograde neurofilament transport. Effect of disruption of dynein/dynactin on the average frequency of neurofilament movement in SCG neurons (A–D) and cortical neurons (E and F) from wild-type mice. Data for each condition are the average of at least 20 15-min movies gathered from at least three different experiments. The anterograde (A) and retrograde (R) frequencies are represented by the top and bottom bars, respectively. (A) Efficiency of RNAi knockdown after 7 d culture (6 d after siRNA injection), determined by immunostaining with an antibody to dynein heavy chain (see Materials and Methods). Control siRNA: cells injected with scrambled siRNA (26 movies). DHC siRNA: cells injected with a pool of three siRNAs targeting dynein heavy chain (21 movies). (B) Effect of dynein heavy chain knockdown on neurofilament movement 6 d after siRNA injection (7 d in culture). Control siRNA: cells injected with scrambled siRNA (23 movies). DHC siRNA: cells injected with a pool of three siRNAs targeting dynein heavy chain (20 movies). (C) Effect of function-blocking dynein intermediate chain antibody IC74.1 on neurofilament movement 2–6 h after antibody injection (5 d in culture). Control antibody (Ab): cells injected with control IgG (38 movies). DIC Ab: cells injected with antibody IC74.1 (20 movies). (D) Effect of p50/dynamitin overexpression on neurofilament movement 3 d after transfection (5 d in culture). Control: untreated cells (59 movies). p50: cells transfected with p50/dynamitin construct (44 movies). (E) Effect of p150-CC1 overexpression on neurofilament movement 2 d after transfection (2 d in culture). Control: untreated cells (26 movies). p150-CC1 (low): cells transfected with 25 μg/ml p150-CC1 construct (23 movies). p150-CC1 (high): cells transfected with 75 μg/ml p150-CC1 construct (20 movies). (F) Effect of p150-CC1 overexpression on neurofilament movement 4 d after transfection (4 d in culture). Control: untreated cells (20 movies). p150-CC1 (low): cells transfected with 25 μg/ml p150-CC1 construct (21 movies). p150-CC1 (high): cells transfected with 75 μg/ml p150-CC1 construct (21 movies). The data in A were compared to the control with a *t* test. The data in B–F were compared to the control with the Mann–Whitney test. p values: ***$p < 0.005$, **$p < 0.01$, and *$p < 0.05$. See Supplemental Tables S3 and S4 for a more detailed summary of these data.

type neurons. Thus, it is possible that there is functional redundancy among the kinesin-1 motors with respect to neurofilament transport and that kinesin-1B and/or kinesin-1C may also be capable of moving neurofilaments in these neurons. The idea that there is functional redundancy among the kinesin-1 isoforms has been proposed previously by Hirokawa and colleagues (Kanai *et al*., 2000), but it remains unproven.

In addition to showing that kinesin-1A is an anterograde neurofilament motor, our data indicate that kinesin-1A is also required for retrograde neurofilament movement. To determine whether this dependence is reciprocal, we inhibited dynein function by using RNA interference, function blocking antibody and overexpression of p50/dynamitin or the CC1 domain of p150. In each case, we observed an inhibition of both retrograde and anterograde movement. Notably, we observed this reciprocal effect with both acute inhibition of dynein (2–6 h after injection of function-blocking antibody) as well as with chronic inhibition (3 d after transfection with dominant negative constructs or 6 d after transfection with dynein heavy chain siRNA). These data differ from the data of the Baas and Black laboratories. In their hands, knockdown of dynein heavy chain by RNA interference in cultured rat SCG neurons reduced the frequency of retrograde neurofilament movement by 92%, yet there was actually a 64% *increase* in the frequency of anterograde movement (He *et al*., 2005). It has also been reported that dynamitin overexpression results in distal accumulations of neurofilaments in cultured rat SCG neurons and PC12 cells (Helfand *et al*., 2003; Ahmad *et al*., 2006), although neurofilament transport was not examined directly in these studies. At present, the explanation for this discrepancy is not clear. The RNAi experiment of Baas and colleagues was performed in rat neurons using different siRNAs, and they also obtained more complete knockdown of dynein heavy chain than we did, but it is not clear how such differences could affect neurofilament transport behavior. Nevertheless, the fact that we have obtained the same result using four independent approaches in two different cell types gives us confidence that our data are not spurious.

Axonal microtubules are orientated uniformly with their plus ends distal (Heidemann *et al*., 1981), so it is clear that kinesin-1 isoforms cannot function as retrograde motors and that dynein cannot function as an anterograde motor. Therefore, the most plausible interpretations of our data are that kinesin-1A is an anterograde motor, that it also somehow activates or enables dynein, and that dynein is a retrograde motor which also functions in a reciprocal capacity for kinesin-1A. In fact, there is considerable evidence that this type of reciprocal dependence is more the rule than the exception for microtubule-based motility. For example, monoclonal antibodies to kinesin-1 or dynactin all inhibit both anterograde and retrograde organelle movement in squid axoplasm (Brady *et al*., 1990; Stenoien and Brady, 1997; Waterman-Storer *et al*., 1997) and mutations in kinesin-1, dynein or dynactin all exhibit general defects in both anterograde and retrograde organelle movement in *Drosophila* larval segmental nerve (Hurd and Saxton, 1996; Martin *et al*., 1999). Knockdown of either kinesin-1 or dynein also inhibits both anterograde and retrograde movement of ribonucleoprotein granules in *Drosophila* S2 cells (Ling *et al*., 2004) and the plus-end–directed movements of lipid droplets in *Drosophila* embryos are severely impaired by mutations in dynein or dynactin (Gross *et al*., 2002).

A central question regarding the mechanism of bidirectional transport in cells is whether motion is the result of a "tug-of-war" between motors of opposite directionality that are simultaneously bound and independently active, or whether the opposing motors are coordinated such that only motors of one directionality are either bound or active at one time (Gross, 2003; Welte, 2004). Our present data on neurofilament transport seem to be inconsistent with a simple tug-of-war model because, in such a model, loss of the anterograde motor should enhance retrograde movement, not impair it (Gross, 2004). In fact, it is particularly striking to us that for every manipulation of either dynein/dynactin or kinesin-1 used in this study, the effect on retrograde movement mirrors the effect on anterograde movement almost exactly, and vice versa (see Figures 2, 4, and 6). This close reciprocal interdependence implies a tight functional coupling between these opposing motors. One possible coupling mechanism is that kinesin and dynein physically interact, either directly or indirectly, to form a dual-motor complex in which both motors must be present for either one to be functional. Such a model has been proposed to explain the bidirectional motion of vesicular cargoes in a variety of systems (Gross, 2003, 2004; Welte, 2004; Shubeita *et al*., 2008). Moreover, a direct interaction between kinesin-1 and dynein has been demonstrated in vitro (Ligon *et al*., 2004), although the functional significance of this interaction remains to be established. Thus, it is possible that dynein and kinesin-1 form dual motor complexes on the surface of each moving neurofilament and that there exists a directional switching mechanism that determines which motor is active. However, it is also possible that the motors are simultaneously active and that the coupling mechanism involves mechanical rather than physical interactions. For example, mathematical modeling of bidirectional transport, taking into account the load dependence of motor properties, has shown that mechanical interactions between opposing motors that are simultaneously active can generate alternating bouts of anterograde and retrograde motion and an interdependence that is at least qualitatively similar to what we observe in our present study (Muller *et al*., 2008). To test these hypotheses, it will be necessary to use super-resolution tracking techniques and/or direct measurements of stall forces under conditions of selective impairment of dynein or kinesin motors. This is currently possible for large membranous organelles (Shubeita *et al*., 2008), but not for neurofilaments.

ACKNOWLEDGMENTS

A. U. performed the kinesin experiments, and N.H.A. performed the dynein experiments. We thank Larry Goldstein (University of California, San Diego) for generously providing the kinesin-1A knockout mice and affinity-purified antisera against kinesin-1A and kinesin-1C; Kitty Jensen in the Brown laboratory for cloning of mouse NFM cDNA and making the GFP fusion construct; Virginia Lee for neurofilament antibodies; Robert Evans (University of Colorado Denver) for the SW13 cells; Erica Holzbaur (University of Pennsylvania) for dynein and dynactin antibodies; Kevin Pfister (University of Virginia) for the IC74.1 antibody used for microinjection; Richard Vallee (Columbia University) for the myc-tagged p50/dynamitin expression construct; and Nick Quintyne (Florida Atlantic University) for the pDsRed-p150-CC1 expression construct. This project was funded by National Institutes of Health grant R01-NS38526 (to A. B.), with additional support provided by National Institutes of Health grant P30-NS045758. A. U. was also supported by grants-in-aid for scientific research in priority areas from the Japan Ministry of Education, Culture, Sports, Science and Technology, and by the Hayashi Memorial Foundation for Female Natural Scientists.

REFERENCES

Ahmad, F. J., He, Y., Myers, K. A., Hasaka, T. P., Francis, F., Black, M. M., and Baas, P. W. (2006). Effects of dynactin disruption and dynein depletion on axonal microtubules. Traffic *7*, 524–537.

Bloom, G. S., Wagner, M. C., Pfister, K. K., and Brady, S. T. (1988). Native structure and physical properties of bovine brain kinesin and identification of the ATP-binding subunit polypeptide. Biochemistry *27*, 3409–3416.

Brady, S. T., Pfister, K. K., and Bloom, G. S. (1990). A monoclonal antibody against kinesin inhibits both anterograde and retrograde fast axonal transport in squid axoplasm. Proc. Natl. Acad. Sci. USA *87*, 1061–1065.

Brown, A. (2000). Slow axonal transport: stop and go traffic in the axon. Nat. Rev. Mol. Cell. Biol. *1*, 153–156.

Brown, A. (2003). Axonal transport of membranous and nonmembranous cargoes: a unified perspective. J. Cell Biol. *160*, 817–821.

Brown, A., Wang, L., and Jung, P. (2005). Stochastic simulation of neurofilament transport in axons: the "stop-and-go" hypothesis. Mol. Biol. Cell *16*, 4243–4255.

DeBoer, S. R. *et al*. (2008). Conventional kinesin holoenzymes are composed of heavy and light chain homodimers. Biochemistry *47*, 4535–4543.

Dillman, J. F., 3rd, and Pfister, K. K. (1994). Differential phosphorylation in vivo of cytoplasmic dynein associated with anterogradely moving organelles. J. Cell Biol. *127*, 1671–1681.

Echeverri, C. J., Paschal, B. M., Vaughan, K. T., and Vallee, R. B. (1996). Molecular characterization of the 50-kD subunit of dynactin reveals function for the complex in chromosome alignment and spindle organization during mitosis. J. Cell Biol. *132*, 617–633.

Francis, F., Roy, S., Brady, S. T., and Black, M. M. (2005). Transport of neurofilaments in growing axons requires microtubules but not actin filaments. J. Neurosci. Res. *79*, 442–450.

Goslin, K., Hannelore, A., and Banker, G. (1998). Rat hippocampal neurons in low-density culture. In: Culturing Nerve Cells, ed. G. Banker and K. Goslin, Cambridge: MIT Press, 339–370.

Gross, S. P. (2003). Dynactin: coordinating motors with opposite inclinations. Curr. Biol. *13*, R320–R322.

Gross, S. P. (2004). Hither and yon: a review of bi-directional microtubule-based transport. Phys. Biol. *1*, R1–R11.

Gross, S. P., Welte, M. A., Block, S. M., and Wieschaus, E. F. (2002). Coordination of opposite-polarity microtubule motors. J. Cell Biol. *156*, 715–724.

He, Y., Francis, F., Myers, K. A., Yu, W., Black, M. M., and Baas, P. W. (2005). Role of cytoplasmic dynein in the axonal transport of microtubules and neurofilaments. J. Cell Biol. *168*, 697–703.

Heidemann, S. R., Landers, J. M., and Hamborg, M. A. (1981). Polarity orientation of axonal microtubules. J. Cell Biol. *91*, 661–665.

Helfand, B. T., Loomis, P., Yoon, M., and Goldman, R. D. (2003). Rapid transport of neural intermediate filament protein. J. Cell Sci. *116*, 2345–2359.

Hirokawa, N., and Takemura, R. (2005). Molecular motors and mechanisms of directional transport in neurons. Nat. Rev. Neurosci. *6*, 201–214.

Hurd, D. D., and Saxton, W. M. (1996). Kinesin mutations cause motor neuron disease phenotypes by disrupting fast axonal transport in *Drosophila*. Genetics *144*, 1075–1085.

Johnson, C. S., Buster, D., and Scholey, J. M. (1990). Light chains of sea urchin kinesin identified by immunoadsorption. Cell Motil. Cytoskeleton *16*, 204–213.

Jung, C., Lee, S., Ortiz, D., Zhu, Q., Julien, J. P., and Shea, T. B. (2005). The high and middle molecular weight neurofilament subunits regulate the association of neurofilaments with kinesin: inhibition by phosphorylation of the high molecular weight subunit. Brain Res. Mol. Brain Res. *141*, 151–155.

Kanai, Y., Okada, Y., Tanaka, Y., Harada, A., Terada, S., and Hirokawa, N. (2000). KIF5C, a novel neuronal kinesin enriched in motor neurons. J. Neurosci. *20*, 6374–6384.

Kozielski, F., Sack, S., Marx, A., Thormahlen, M., Schonbrunn, E., Biou, V., Thompson, A., Mandelkow, E. M., and Mandelkow, E. (1997). The crystal structure of dimeric kinesin and implications for microtubule-dependent motility. Cell *91*, 985–994.

Kuznetsov, S. A., Vaisberg, E. A., Shanina, N. A., Magretova, N. N., Chernyak, V. Y., and Gelfand, V. I. (1988). The quaternary structure of bovine brain kinesin. EMBO J. *7*, 353–356.

Lakadamyali, M., Rust, M. J., Babcock, H. P., and Zhuang, X. (2003). Visualizing infection of individual influenza viruses. Proc. Natl. Acad. Sci. USA *100*, 9280–9285.

Leopold, P. L., Kreitzer, G., Miyazawa, N., Rempel, S., Pfister, K. K., Rodriguez-Boulan, E., and Crystal, R. G. (2000). Dynein- and microtubule-mediated translocation of adenovirus serotype 5 occurs after endosomal lysis. Hum. Gene Ther. *11*, 151–165.

Ligon, L. A., Tokito, M., Finklestein, J. M., Grossman, F. E., and Holzbaur, E. L. (2004). A direct interaction between cytoplasmic dynein and kinesin I may coordinate motor activity. J. Biol. Chem. *279*, 19201–19208.

Ling, S. C., Fahrner, P. S., Greenough, W. T., and Gelfand, V. I. (2004). Transport of Drosophila fragile X mental retardation protein-containing ribonucleoprotein granules by kinesin-1 and cytoplasmic dynein. Proc. Natl. Acad. Sci. USA *101*, 17428–17433.

Martin, M., Iyadurai, S. J., Gassman, A., Gindhart, J. G., Jr., Hays, T. S., and Saxton, W. M. (1999). Cytoplasmic dynein, the dynactin complex, and kinesin are interdependent and essential for fast axonal transport. Mol. Biol. Cell *10*, 3717–3728.

Martys, J. L., Ho, C.-L., Liem, R.K.H., and Gundersen, G. G. (1999). Intermediate filaments in motion: observations of intermediate filaments in cells using green fluorescent protein-vimentin. Mol. Biol. Cell *10*, 1289–1295.

Melkonian, K. A., Maier, K. C., Godfrey, J. E., Rodgers, M., and Schroer, T. A. (2007). Mechanism of dynamitin-mediated disruption of dynactin. J. Biol. Chem. *282*, 19355–19364.

Muller, M. J., Klumpp, S., and Lipowsky, R. (2008). Tug-of-war as a cooperative mechanism for bidirectional cargo transport by molecular motors. Proc. Natl. Acad. Sci. USA *105*, 4609–4614.

Navone, F., Niclas, J., Hom-Booher, N., Sparks, L., Bernstein, H. D., McCaffrey, G., and Vale, R. D. (1992). Cloning and expression of a human kinesin heavy chain gene: interaction of the COOH-terminal domain with cytoplasmic microtubules in transfected CV-1 cells. J. Cell Biol. *117*, 1263–1275.

Niclas, J., Navone, F., Hom-Booher, N., and Vale, R. D. (1994). Cloning and localization of a conventional kinesin motor expressed exclusively in neurons. Neuron *12*, 1059–1072.

Prahlad, V., Helfand, B. T., Langford, G. M., Vale, R. D., and Goldman, R. D. (2000). Fast transport of neurofilament protein along microtubules in squid axoplasm. J. Cell Sci. *113*, 3939–3946.

Prahlad, V., Yoon, M., Moir, R. D., Vale, R. D., and Goldman, R. D. (1998). Rapid movements of vimentin on microtubule tracks: kinesin-dependent assembly of intermediate filament networks. J. Cell Biol. *143*, 159–170.

Quintyne, N. J., and Schroer, T. A. (2002). Distinct cell cycle-dependent roles for dynactin and dynein at centrosomes. J. Cell Biol. *159*, 245–254.

Roy, S., Coffee, P., Smith, G., Liem, R.K.H., Brady, S. T., and Black, M. M. (2000). Neurofilaments are transported rapidly but intermittently in axons: implications for slow axonal transport. J. Neurosci. *20*, 6849–6861.

Sarria, A. J., Lieber, J. G., Nordeen, S. K., and Evans, R. M. (1994). The presence or absence of a vimentin-type intermediate filament network affects the shape of the nucleus in human SW-13 cells. J. Cell Sci. *107*, 1593–1607.

Shah, J. V., Flanagan, L. A., Janmey, P. A., and Leterrier, J.-F. (2000). Bidirectional translocation of neurofilaments along microtubules mediated in part by dynein/dynactin. Mol. Biol. Cell *11*, 3495–3508.

Shubeita, G. T., Tran, S. L., Xu, J., Vershinin, M., Cermelli, S., Cotton, S. L., Welte, M. A., and Gross, S. P. (2008). Consequences of motor copy number on the intracellular transport of kinesin-1-driven lipid droplets. Cell *135*, 1098–1107.

Stenoien, D. L., and Brady, S. T. (1997). Immunochemical analysis of kinesin light chain function. Mol. Biol. Cell *8*, 675–689.

Tanaka, M., and Herr, W. (1990). Differential transcriptional activation by Oct-1 and Oct-2, interdependent activation domains induce Oct-2 phosphorylation. Cell *60*, 375–386.

Tanaka, Y., Kanai, Y., Okada, Y., Nonaka, S., Takeda, S., Harada, A., and Hirokawa, N. (1998). Targeted disruption of mouse conventional kinesin heavy chain, kif5B, results in abnormal perinuclear clustering of mitochondria. Cell *93*, 1147–1158.

Trivedi, N., Jung, P., and Brown, A. (2007). Neurofilaments switch between distinct mobile and stationary states during their transport along axons. J. Neurosci. *27*, 507–516.

Uchida, A., and Brown, A. (2004). Arrival, reversal and departure of neurofilaments at the tips of growing axons. Mol. Biol. Cell *15*, 4215–4225.

Vorobjev, I., Malikov, V., and Rodionov, V. (2001). Self-organization of a radial microtubule array by dynein-dependent nucleation of microtubules. Proc. Natl. Acad. Sci. USA *98*, 10160–10165.

Wagner, O. I., Ascano, J., Tokito, M., Leterrier, J. F., Janmey, P. A., and Holzbaur, E. L. (2004). The interaction of neurofilaments with the microtubule motor cytoplasmic dynein. Mol. Biol. Cell *15*, 5092–5100.

Wang, L., and Brown, A. (2001). Rapid intermittent movement of axonal neurofilaments observed by fluorescence photobleaching. Mol. Biol. Cell *12*, 3257–3267.

Wang, L., Ho, C.-L., Sun, D., Liem, R.K.H., and Brown, A. (2000). Rapid movement of axonal neurofilaments interrupted by prolonged pauses. Nat. Cell Biol. *2*, 137–141.

Waterman-Storer, C. M., Karki, S. B., Kuznetsov, S. A., Tabb, J. S., Weiss, D. G., Langford, G. M., and Holzbaur, E. L. (1997). The interaction between cytoplasmic dynein and dynactin is required for fast axonal transport. Proc. Natl. Acad. Sci. USA *94*, 12180–12185.

Welte, M. A. (2004). Bidirectional transport along microtubules. Curr. Biol. *14*, R525–R537.

Windoffer, R., and Leube, R. E. (1999). Detection of cytokeratin dynamics by time-lapse fluorescence microscopy in living cells. J. Cell Sci. *112*, 4521–4534.

Xia, C., Rahman, A., Yang, Z., and Goldstein, L. S. (1998). Chromosomal localization reveals three kinesin heavy chain genes in mouse. Genomics *52*, 209–213.

Xia, C. H., Roberts, E. A., Her, L. S., Liu, X., Williams, D. S., Cleveland, D. W., and Goldstein, L. S. (2003). Abnormal neurofilament transport caused by targeted disruption of neuronal kinesin heavy chain KIF5A. J. Cell Biol. *161*, 55–66.

Yabe, J. T., Jung, C. W., Chan, W.K.H., and Shea, T. B. (2000). Phospho-dependent association of neurofilament proteins with kinesin in situ. Cell Motil. Cytoskeleton *45*, 249–262.

Yabe, J. T., Pimenta, A., and Shea, T. B. (1999). Kinesin-mediated transport of neurofilament protein oligomers in growing axons. J. Cell Sci. *112*, 3799–3814.

Yan, Y., and Brown, A. (2005). Neurofilament polymer transport in axons. J. Neurosci. *25*, 7014–7021.